

SPM—SEM Investigations of Semiconductor Nanowires for Integrated Metal Oxide Gas Sensors [†]

Verena Leitgeb ^{1,*}, Katrin Fladischer ¹, Frank Hitzel ², Florentyna Sosada-Ludwikowska ¹, Johanna Krainer ¹, Robert Wimmer-Teubenbacher ¹ and Anton Köck ¹

¹ Materials for Microelectronics, Materials Center Leoben Forschung GmbH, 8700 Leoben, Austria; katrin.fladischer@mcl.at (K.F.); florentyna.sosada-ludwikowska@mcl.at (F.S.-L.); johanna.krainer@gmail.com (J.K.); robert.wimmer-teubenbacher@mcl.at (R.W.-T.); anton.koeck@mcl.at (A.K.)

² Semilab Germany GmbH, 38106 Braunschweig, Germany; frank.hitzel@semilab.com

* Correspondence: verena.leitgeb@mcl.at; Tel.: +43-3842-45922-79

[†] Presented at the Eurosensors 2018 Conference, Graz, Austria, 9–12 September 2018.

Published: 4 December 2018

Abstract: Integration of metal oxide nanowires in metal oxide gas sensors enables a new generation of gas sensor devices, with increased sensitivity and selectivity. For reproducible and stable performance of next generation sensors, the electric properties of integrated nanowires have to be well understood, since the detection principle of metal oxide gas sensors is based on the change in electrical conductivity during gas exposure. We study two different types of nanowires that show promising properties for gas sensor applications with a Scanning Probe Microscope—Scanning Electron Microscope combination. Electron Beam Induced Current and Kelvin Probe Force Microscopy measurements with a lateral resolution in the nanometer regime are performed. Our work offers new insights into the dependence of the nanowire work function on its composition and size, and into the local interaction between electron beam and semiconductor nanowires.

Keywords: metal oxide nanowire; scanning probe microscope—scanning electron microscope combination; kelvin probe force microscopy; electron beam induced current

1. Introduction

For realization of next generation gas sensor devices based on integrated semiconductor nanowires (NWs), the effects of NW geometry and composition on their electric properties must be well understood. The detection principle of metal oxide gas sensors is based on the change in electrical conductivity during gas exposure and can be greatly enhanced in terms of sensitivity and selectivity by applying integrated nanowires [1–3].

We characterize two different types of NWs that show promising properties for gas sensor applications, n-type silicon dioxide (SnO₂) and p-type copper oxide (CuO) semiconducting NWs [4]. For characterization and analysis of semiconducting materials, Scanning Electron Microscopy (SEM) and Scanning Probe Microscopy (SPM) are established tools. By using a combined SPM-SEM system, advanced studies on local electric properties can be performed [5]. We perform Kelvin Probe Force Microscopy (KPFM) and Electron Beam Induced Current (EBIC) measurements to study the relation between NW geometry and work function, and the local interaction between n- and p-type semiconductor NWs and the SEM electron beam, respectively.

KPFM shows the difference in work function between n-type SnO₂ and p-type CuO NWs, and how the NW work function shifts with decreasing NW diameter. EBIC measurements show different electric

behavior of n- type and p- type semiconductor nanowires for large (micrometer) distances between electron beam and SPM-probe. For submicron distances, however, the current signals assimilate.

2. Materials and Methods

N-type SnO₂ NWs are grown by vapor phase decomposition and p-type CuO NW are grown by thermal oxidation process. A stamp is used to transfer the NWs to their respective substrates. For KPFM, a silicon dioxide (SiO₂) substrate with a 2 nm conductive chromium (Cr) layer coated by thermal evaporation is used. EBIC measurements are performed on an insulation substrate, consisting of a top layer of 1300 nm thick SiO₂ on silicon nitride (SiN).

Nanowire characterization is performed inside a SPM-SEM combination (BRR 2770 from DME (Nowadays commercially available as AFM Option for Carl Zeiss FE-SEMs), SEM-FIB Auriga 40 from Zeiss). To get nm-resolved information on the electric properties of the NWs, we apply KPFM, and EBIC measurements. KPFM works in non-contact mode and gives the WF of local surface structures by measuring the potential offset between SPM-probe and sample surface. For KPFM we use an Arrow-NCPT probe. EBIC is a versatile SEM technique based on the injection of charge carriers, the measurement principle is outlined in Figure 1. The SPM-probe (PPP- CONTPt) is placed on selected NWs and works as current detector. While the SPM-probe stays fixed, the electron beam focus point (diameter ~1 nm) is varied along the NW. To ensure a stable signal, we measure the current on each point for about 10 seconds. EBIC experiments are performed at ambient temperature inside the SEM vacuum chamber at $\sim 2 \times 10^{-6}$ mbar. No external bias voltage is applied in our setup. The SPM is tilted at an angle of 63° (an angle of 0° is perpendicular, 90° is parallel to the electron beam), with an initial energy of the electron beam of 5 keV. The tilting is necessary to visualize the SPM-probe; otherwise, the SPM cantilever would shadow the probe.

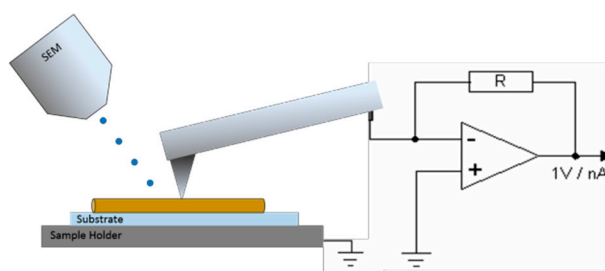


Figure 1. Sketch of the EBIC measurement setup inside the SPM-SEM combination.

3. Results

For KPFM analysis of NWs, see Figure 2, we use the difference in potential between NW and the Cr substrate, as the potential of the SPM-probe is subject to changes due to abrasion or picking up of alien material.

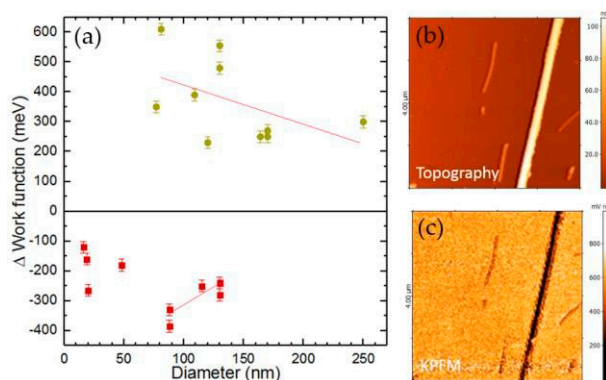


Figure 2. (a) Difference in WF between SnO₂ NWs and the Cr substrate (dark yellow circles), and CuO NWs and Cr (red squares). Red lines are linear fits; (b) Topography and (c) KPFM image ($4 \times 4 \mu\text{m}^2$) of a representative CuONW.

For SnO₂NWs, the mean difference in WF with respect to the Cr substrate amounts to $\Delta WF = 370 \text{ meV} \pm 40 \text{ meV}$, measured over NWs with diameters from 70 nm to 250 nm. For CuO NW, the mean WF difference with respect to the Cr substrate amounts to $\Delta WF = -245 \text{ meV} \pm 30 \text{ meV}$. For CuO NW, the measured diameters vary between 16 nm and 130 nm. NW height (diameter) is measured out of profiles through topography images recorded simultaneously with the KPFM signal. For SnO₂NWs, we observe a decrease in ΔWF with increasing NW diameter. For CuO NW, however, an increase in ΔWF with increasing NW diameter is observed, but only for CuO NW with diameter >70 nm. For smaller CuO NW, WF values scatter strongly.

For EBIC characterization, we place the SPM-probe on one end of a SnO₂, respectively CuO NW. While the SPM-probe stays fixed, the electron beam focus point is varied along the NW and the current induced by the electron beam is measured via the SPM-probe (see Figure 3). For the SnO₂ NW, a quite stable positive current of about 30 pA is observed for beam-probe distances larger than 500 nm up to the end of the NW. For the CuO NW, negative current is measured, which decreases from about -30 pA at larger (>500 nm) beam-probe distances, to down to -70 pA at small beam-probe distances. The same current decrease for beam-probe distances <500 nm is also observed for the SnO₂ NW, with values down to -100 pA at 200 nm beam-probe distance. No beam-probe distances larger than 1.5 μm are measured for the CuO NW due to the smaller length of the NW.

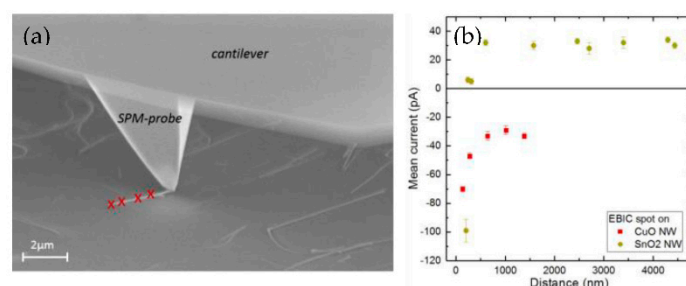


Figure 3. (a) SPM-probe placed on CuO NW, red crosses are exemplary positions of electron beam focus points on the CuO NW; (b) EBIC measurement on SnO₂ NWs (dark yellow circles) and CuO NWs (red squares). Distances measured along the direct path between electron beam focus point and SPM-probe.

4. Discussion

KPFM shows difference in WF between SnO₂ and CuO NW of about 600 meV. Interestingly, the measured surface potentials of SnO₂ and CuO NW are located above and beneath that of the Cr substrate. This is different to the material's bulk values, where the Fermi levels of both SnO₂ and CuO are both located beneath the Fermi level of Cr. We suspect the cause is that for nanoscale structures, like NW, surface states and defects play a more important role, and the carrier concentration strongly increases. For the n-type SnO₂ NW, a higher carrier concentration will increase the Fermi level, for the p-type CuO NW, a higher carrier concentration will decrease it. This shift the Fermi level of the SnO₂ NW above the Fermi level of Cr, and also leads to the measured decrease/increase in ΔWF with increasing NW diameter for SnO₂/CuO NWs. The strong scattering CuO NWs <50 nm in diameter might be due to insufficient growth times of shorter NW, which cause different morphology [6].

The measured positive (SnO₂ NW) or negative (CuO NW) EBIC values at large beam-probe distances can be explained by taking the band structures of the SPM-probe and the NWs into account. For SnO₂, being an n-type semiconductor, electrons are the majority charge carriers. The structure of the conduction band E_c dictates that transport of negative charges takes place from sample to probe (defined as positive current). For CuO, being a p-type semiconductor, holes are the majority charge carrier. Here, the structure of the valence band E_v dictates transport of positive charges from sample to probe. See Figure 4 for a sketch of the band structures. For small beam-probe distances <500 nm, the SPM-probe interacts with the intrinsic region formed in the semiconductor due to E-beam irradiation. Due to the positive charging of the SiO₂ substrate [7], the negative charges inside the intrinsic region of the NW accumulate at the bottom of the NW near the SiO₂ substrate, while the

positive charge accumulates in the NW top region. This applies for both NW types. The SPM-probe sits directly over the charge separated intrinsic region of the semiconductor and as a result, negative currents are measured for small beam-probe distances.

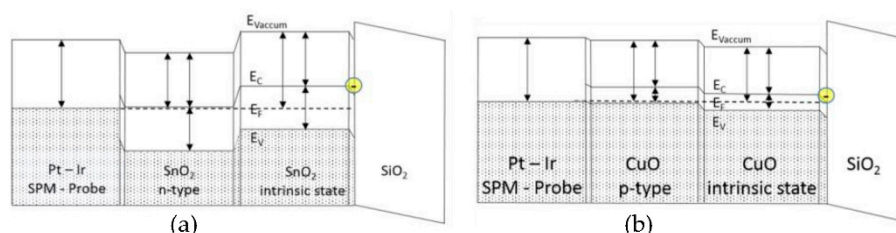


Figure 4. Band structure of the SPM-probe placed on (a) SnO₂ NW and (b) CuO NW on SiO₂ substrate, with E_c the conduction band, E_v the valence band, and E_f the Fermi level.

5. Conclusions

Characterization of semiconductor NWs in a combined SPM-SEM system reveals how the NW work function depends on composition and NW size. Results of EBIC measurements show different electric behavior of n- type and p- type semiconductor nanowires for large (>0.5 μm) distances between electron beam and SPM-probe. For submicron distances, the current signals assimilate. Our work offers new insights into the local electrical behavior of semiconductor nanowires and their functionality as gas sensing material.

Author Contributions: V.L., K.F., and A.K. conceived and designed the experiments; V.L. and K.F. performed the experiments; V.L., K.F. and R.W.-T. analyzed the data; F.S.-L. and J.K. contributed materials; F.H. contributed analysis tools and helped with data interpretation; V.L. wrote the paper.

Acknowledgments: This work was performed within the project “FunkyNano—Optimized Functionalization of Nanosensors for Gas Detection by Screening of Hybrid Nanoparticles” funded by the FFG—Austrian Research Promotion Agency (Project No. 858637).

Conflicts of Interest: The authors declare no conflict of interest. The founding sponsors had no role in the design of the study; in the collection, analyses, or interpretation of data; in the writing of the manuscript, and in the decision to publish the results.

References

1. Barsan, N.; Koziej, D.; Weimar, U. Metal oxide-based gas sensor research: How to? *Sens. Actuators B Chem.* **2007**, *121*, 18–35. doi:10.1016/j.snb.2006.09.047
2. Wimmer-Teubenbacher, R.; Lackner, E.; Krainer, J.; Steinhauer, S.; Koeck, A. Gas Sensor Devices based on CuO- and ZnO- Nanowires directly synthesized on silicon substrate. *MRS Adv.* **2016**, *1*, 817–823. doi:10.1557/adv.2016.241
3. Comini, E.; Sberveglieri, G. Metal oxide nanowires as chemical sensors. *Mater. Today* **2010**, *13*, 36–44. doi:10.1016/S1369-7021(10)70126-7
4. Kolmakov, A.; Zhang, Y.; Cheng, G.; Moskovits, M. Detection of CO and O₂ using tin oxide nanowire sensors. *Adv. Mater.* **2003**, *15*, 997–1000. doi:10.1002/adma.200304889
5. Heiderhoff, R.; Cramer, R.M.; Balk, L.J. High resolution electron beam induced current measurements in an SEM-SPM hybrid system by tip induced barriers. *Inst. Phys. Conf. Ser.* **1995**, *149*, 189–194.
6. Chen, J.T.; Zhang, F.; Wang, J. CuO nanowires synthesized by thermal oxidation route. *J. Alloys Compd.* **2008**, *454*, 268–273. doi:10.1016/j.jallcom.2006.12.032
7. Glavatskikh, I.A.; Kortov, V.S.; Fitting, H.J. Self-consistent electrical charging of insulating layers and metal- insulator-semiconductor structures. *J. Appl. Phys.* **2001**, *89*, 440–448. doi:10.1063/1.1330242

